Electron-phonon coupling and superconductivity in the light actinides: A first-principles study

P. González-Castelazo,[1] R. de Coss-Martínez,[1] O. De la Peña-Seaman,[1,2] R. Heid,[2] and K.-P. Bohnen[2]

[1]*Instituto de Física, Benemérita Universidad Autónoma de Puebla, Apartado Postal J-48 C.P. 72570 Puebla, Puebla, México*

[2]*Karlsruher Institut für Technologie (KIT), Institut für Festkörperphysik P.O. Box 3640, D-76021 Karlsruhe, Germany*

A systematic investigation of electronic, lattice dynamical, and superconducting properties of the early actinides Ac, Th, and Pa within the framework of density functional perturbation theory is presented. Spin-orbit coupling is included self-consistently in the calculation of all relevant quantities. The largest coupling constant is obtained for Ac, which with $\lambda \approx 0.97$ is close to the strong coupling regime, and where a sizable superconducting transition temperature of 4–5 K is predicted. For Th and Pa, a reduced $\lambda \approx 0.5$ is found in accordance with the observed smaller T_c. By comparing with scalar-relativistic calculations we found that spin-orbit coupling results in a hardening of the phonon spectrum for all cases. Its influence on λ is almost negligible for Ac and Pa. In contrast, for Th spin-orbit interaction invokes band splittings near the Fermi level, which reduces λ by 21%.

I. INTRODUCTION

The light actinides, from Ac to Pu, represent a challenge to contemporary electronic structure theories and methodologies. The presence of itinerant and highly directional f electrons plays an important role in the bonding and also on the density of states at the Fermi level. Such characteristics drive, among other effects, the formation of vast, different, and sometimes complex crystal structures as well as intricate electronic interactions and correlations. Besides, the light actinides possess a massive nucleus that induces significant relativistic corrections in the electronic structure. A theoretical description thus requires by norm to take into account the spin-orbit interaction. Despite these challenges, there are in literature several theoretical investigations devoted to structural and electronic properties of the light actinides [1–7]. However, the reported findings are quite diverse and far from being conclusive, even for the simplest elements of the series, like for example Th. The vibrational properties have been studied by inelastic neutron scattering and inelastic x-ray scattering for Th [8], U [9–11], and Pu [12]. The main target of these studies was to establish stability criteria and to understand phase transitions in those heavy elements, with the aim to control them for further application to nuclear energy. From a theoretical point of view, only a few attempts have been made on $5f$ systems applying the most advanced, accurate, and state-of-the-art techniques nowadays, such as density functional perturbation theory (DFPT) [13]. Among the light actinides, most studies were devoted to Th [14–17]. U has also attracted some attention [14,18], however, a microscopic analysis is more involved due to its complex crystal structure (orthorhombic at low temperatures) and the active participation of $5f$ electrons in the bonding. The results from calculations are, in general, in agreement with experimental data, like for example the appearance of phonon anomalies and the range of frequencies. However, a deeper analysis of whether or not the observed anomalies are affected or even driven by spin-orbit coupling (SOC) is still lacking. Similarly, it is unknown to what extend SOC influences the phonon spectrum, the structural stability, and possibly also the observed phase transitions in the light actinides.

Among the different properties studied for the light actinides, the most intriguing and interesting ones are super-conductivity and the electron-phonon (e-ph) coupling as the most likely pairing mechanism. Experimentally, many of the light actinides are superconductors, but with very small critical temperature (T_c) ranging from 1.4 K for Th, to 0.001 K for Pu [19,20]. Information about the coupling properties is scarce. Estimates of the electron-phonon coupling parameter (λ) were obtained by simple inversion of the T_c McMillan formula [21]. With an assumed value of 0.13 for the Coulomb pseudopotential μ^*, λ for the light actinides ranges from 0.54 for Th, to 0.26 for Pu [20], which put them into the medium to weak coupling regime. From the theory side, only a small number of papers were devoted to the e-ph coupling of the $5f$ systems [19,20,22] so far, mainly because proper models and theories capable of dealing with them were lacking. Skriver *et al.* [20] presented a systematic study of the e-ph coupling of the light actinides series. In that study, SOC was explicitly taken into account only for the electronic structure, while its impact on lattice dynamics was treated indirectly via an experimental Debye temperature. E-ph coupling properties were calculated using the Gaspary-Gyorffi theory [23]. Results for the coupling constants showed good agreement with those deduced from experimental data in some cases, like for Th or Pu, while in other cases the differences were very large (as for Pa or U). A very interesting outcome from the Skriver calculations was the prediction of a very large e-ph coupling for Ac, $\lambda = 1.655$, which would be higher than the highest one for a single element in the periodic table known to date (1.6 for Hg). Unfortunately, no experiments have been carried out to verify this prediction so far, because Ac is a rare and expensive element, and in addition highly radioactive and poisonous.

In this paper, we present a study of the electronic properties, lattice dynamics, e-ph and superconductivity of light actinides (Ac, Th, Pa) within the framework of density functional theory (DFT) [24]. In particular, we calculate the electronic band structure applying DFT methods, and phonon dispersion within density functional perturbation theory (DFPT) formalism [13]. The quantities determined by DFPT calculation allow a straightforward evaluation of the microscopic e-ph interaction, which are required as an input to the strong-coupling Eliashberg theory [25]. We obtain the e-ph properties such as the Eliashberg function, $\alpha^2 F(\omega)$, and the e-ph coupling constant λ. Superconducting critical temperatures T_c are

104512-1

obtained by solving the linearized Eliashberg gap equations in the isotropic limit. The effect of SOC on these quantities is systematically analyzed and discussed in connection with the electronic and vibrational properties.

The paper is organized as follows. In Sec. II, the details of the computational method are described. Results for structural and electronic properties are given is Secs. III A and III B, respectively, while lattice dynamical properties are discussed in Sec. III C. Finally, the electron-phonon coupling and superconducting properties are analyzed in Sec. III D, followed by concluding remarks in Sec. IV.

II. COMPUTATIONAL DETAILS

The calculations were performed with the mixed-basis pseudopotential method (MBPP) [26,27] including the spin-orbit interaction [28,29]. In this method, valence states are expanded in a combination of plane waves and localized functions centered at atomic sites. The latter improves the description of wave functions, which are more localized near an atomic site, and allows a significant reduction of the basis set without sacrificing the accuracy. For light actinides (Ac, Th, Pa) norm-conserving pseudopotentials were constructed according to the Vanderbilt description [30], delivering both scalar-relativistic and SOC components of the pseudopotential [28,29]. Partial core corrections have been included and we have explicitly considered $5d$ semicore states as valence states. Local functions of d and f type at each atomic site were supplemented by plane waves up to a kinetic energy of 30 Ry. Phonon properties were calculated via density-functional perturbation theory (DFPT) [13] as implemented in the MBPP code [31,32]. The DFPT has been successfully applied to heavy elements, which usually require the inclusion of SOC, like Pb, Bi, and Tl [28,29,33], where the dispersion curves showed excellent agreement with experimental results (see Ref. [28] and references therein for more details of the implementation). The present study was carried out with the generalized gradient approximation (GGA) in the parametrization of PBE [34,35] for the exchange-correlation functional. Brillouin zone integration was performed using Monkhorst-Pack special k-point sets with a Gaussian smearing of 0.2 eV [36]. For the calculations of ground state properties (structural optimization and electronic properties) as well as phonons we used a $16 \times 16 \times 16$ k-point mesh. Dynamical matrices were calculated on a $8 \times 8 \times 8$ q-point mesh for Ac and Th with the fcc structure and on a $4 \times 4 \times 4$ q-point mesh for bct Pa. Complete phonon dispersions were then obtained via standard Fourier interpolation. For the calculations of electron-phonon coupling matrix elements, a denser k-point mesh of $32 \times 32 \times 32$ was required for both structures.

With the knowledge of phonon dispersion and the e-ph matrix elements we calculated the Eliashberg function,

$$\alpha^2 F(\omega) = \frac{1}{2\pi \hbar N(E_F)} \sum_{\mathbf{q}\lambda} \frac{\gamma_{\mathbf{q}\lambda}}{\omega_{\mathbf{q}\lambda}} \delta(\omega - \omega_{\mathbf{q}\lambda}), \quad (1)$$

where $N(E_F)$ is the electronic density of states at the Fermi level (per atom and spin), $\omega_{\mathbf{q}\lambda}$ denotes the frequency of the phonon mode ($\mathbf{q}\lambda$), and $\gamma_{\mathbf{q}\lambda}$ is defined as

$$\gamma_{\mathbf{q}\lambda} = 2\pi \omega_{\mathbf{q}\lambda} \sum_{\mathbf{k}\nu\nu'} \left| g^{\mathbf{q}\lambda}_{\mathbf{k}+\mathbf{q}\nu',\mathbf{k}\nu} \right|^2 \delta(\epsilon_{\mathbf{k}\nu} - E_F)\delta(\epsilon_{\mathbf{k}+\mathbf{q}\nu'} - E_F).$$
$$(2)$$

$\epsilon_{\mathbf{k}\nu}$ represent the one-electron band energies with momentum $\mathbf{k}$ and band index ν. g is the e-ph coupling matrix element for scattering of an electron from a Bloch state with momentum $\mathbf{k}\nu$ to another Bloch state $\mathbf{k} + \mathbf{q}\nu'$ by a phonon $\mathbf{q}\lambda$, and is given by

$$g^{\mathbf{q}\lambda}_{\mathbf{k}+\mathbf{q}\nu',\mathbf{k}\nu} = \sqrt{\frac{\hbar}{2\omega_{\mathbf{q}\lambda}}} \sum_{\kappa a} \frac{1}{\sqrt{M_\kappa}} \eta^{\mathbf{q}\lambda}_{\kappa a} \langle \mathbf{k} + \mathbf{q}\nu' | \delta^{\mathbf{q}}_{\kappa a} V | \mathbf{k}\nu \rangle, \quad (3)$$

where M_κ is the mass of the κth atom in the unit cell and $\eta^{\mathbf{q}\lambda}_{\kappa a}$ is the normalized eigenvector of the phonon mode ($\mathbf{q}\lambda$). The term $\delta^{\mathbf{q}}_{\kappa a} V$ denotes the first-order change in the total crystal potential with respect to the displacement of the atom κ in the a direction. The average e-ph coupling constant (λ) is related to the Eliashberg function as

$$\lambda = 2 \int_0^\infty \frac{d\omega}{\omega} \alpha^2 F(\omega) = \frac{1}{\pi \hbar N(E_F)} \sum_{\mathbf{q}\lambda} \frac{\gamma_{\mathbf{q}\lambda}}{\omega^2_{\mathbf{q}\lambda}}. \quad (4)$$

Another useful integrated quantity is the average effective frequency defined by

$$\omega_{\log} = \exp\left(\frac{2}{\lambda} \int_0^\infty d\omega \frac{\ln(\omega)}{\omega} \alpha^2 F(\omega) \right), \quad (5)$$

which sets the energy scale for the transition temperature. Finally, the calculated $\alpha^2 F(\omega)$ are used to obtain estimates for the critical temperature (T_c) by solving numerically the linearized Eliashberg gap equations [25,37–39].

III. RESULTS AND DISCUSSION

A. Structural properties

The studied light actinides possess different ground-state crystal structures (α-phase). While Ac and Th crystallize in an fcc structure, Pa has a body-center tetragonal (bct) lattice. Structural optimizations were performed both on the scalar-relativistic (SR) level and by including spin-orbit coupling (SOC). Results for equilibrium volume and bulk modulus are shown in Table I and compared with previous calculations and experimental data.

In all cases the inclusion of SOC leads to a small reduction of the equilibrium volume and a slight increase of the bulk modulus, with largest differences of $\approx 2\%$ and 6%, respectively. Our values agree well with those obtained with all-electron techniques [6,7] for Th and Pa. For Ac, as no such study exists so far, we performed our own LAPW calculations [49] and found again very good agreement with our MBPP results for both V_0 and B_0. This consistency with all-electron methods ensures the good quality of the employed pseudopotentials.

Comparison with experimental data exhibits two noticeable discrepancies. Our calculated equilibrium volume for Ac exceeds the experimental one by more than 20%. Part of the discrepancy could, on one hand, be due to the use of GGA, which tends to underbind a crystal, but on the other hand, the only reported experimental value was obtained under

TABLE I. Equilibrium volume (in units of a_B^3, where a_B denotes the Bohr radius) and bulk modulus (in GPa) for the light actinides Ac, Th (fcc), and Pa (bct). Present results from structural optimization without (SR) and with (SOC) spin-orbit coupling are compared with all-electron GGA calculations (Theory) and experimental studies (Expt.).

			This work	Theory	Expt.
Ac	V_0	SR	310.18	308.08[a]	252.7[b]
		SOC	303.66	304.51[a]	
	B_0	SR	24.21	23.18[a]	
		SOC	25.26	25.20[a]	
Th	V_0	SR	219.32	219.3[c],216.9[d],218.0[f]	221.7[e]
		SOC	215.49	218.1[c],214.8[d],216.7[f]	
	B_0	SR	54.85	56.7[c],58.8[d]	
		SOC	58.02	73.1[c],63.4[d]	58[g]
Pa	V_0	SR	168.80	169.3[c],168.7[d]	168.30[h]
		SOC	167.11	168.4[c],169.9[d]	
	c/a	SR	0.8135		0.825[h]
		SOC	0.8178		
	B_0	SR	91.01	105[c],95[d]	157[i]
		SOC	92.21	105[c],97[d]	

[a]present LAPW calculations, see text and Ref. [49].
[b]298 K, Ref. [40].
[c]LAPW, Ref. [6].
[d]Gaussian, Ref. [6].
[e]298 K, Ref. [41].
[f]LAPW, Ref. [7].
[g]298 K, Ref. [42].
[h]298 K, Ref. [43].
[i]298 K, Ref. [44].

difficult conditions for a multiphase sample [40]. A second larger discrepancy is found for the bulk modulus of Pa. Here, measurements were performed at room temperature, and no low temperature value is known.

B. Electronic properties

The electronic band structures and density of states (DOS) of Ac, Th, and Pa are presented in Fig. 1 for both SR and SOC calculations (each performed at the corresponding optimized lattice structure). The largest effect of SOC is a splitting of the low-lying $6p$ states far below E_F (at ≈ -25 eV, not shown here) [7]. However, SOC-induced modifications can also be seen in the region close to E_F. For Ac and Th, band splittings occur at the W point, along the W-L high-symmetry direction, and along the Γ-K direction. For Pa larger changes are evident in the vicinity of the P point. The affected bands have primarily d and f character, albeit their relative weight depends on the specific element. For Ac they are exclusively built from d states, while for Th they have a mixed d and f character. In the case of Pa the dominant contribution comes from f states.

As seen in the right panels in Fig. 1, the influence of SOC on the density of states, in particular close to the Fermi energy (E_F), is rather minor. A noticeable difference of the DOS at E_F is only found for Th, which is reduced by approximately 10% when SOC is included. This will play a certain role for the electron-phonon coupling as discussed below.
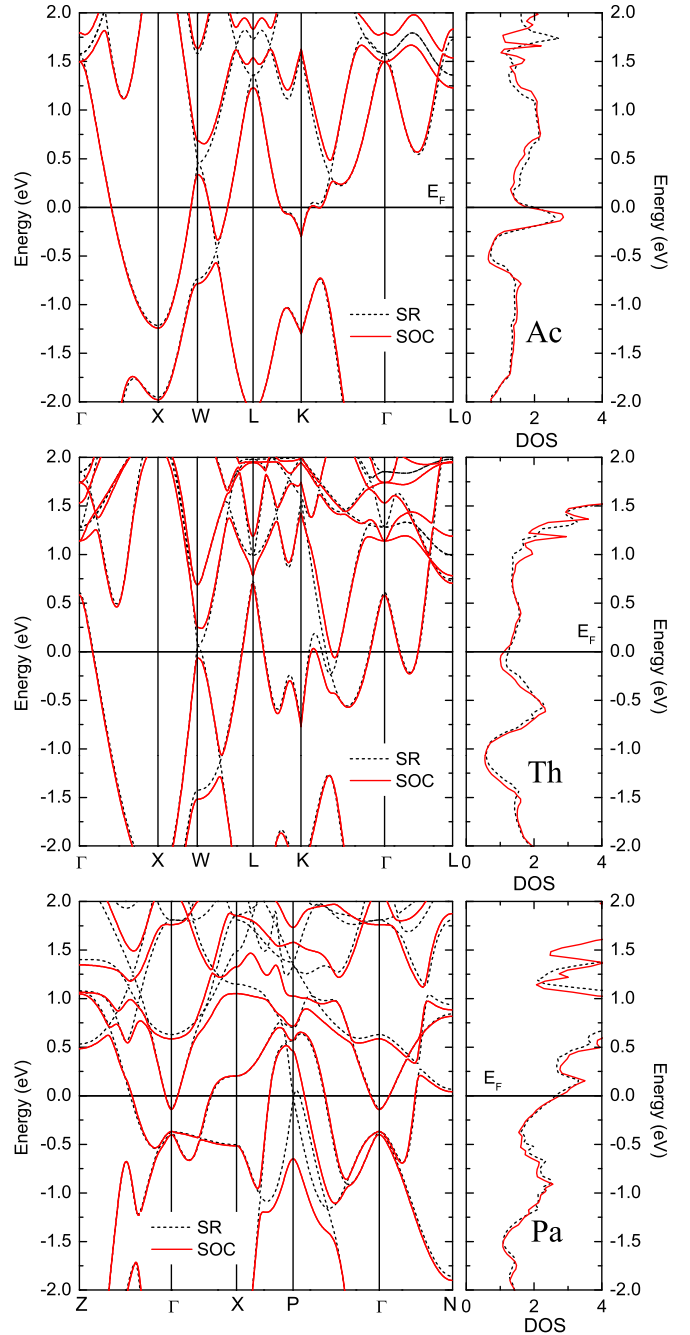
FIG. 1. Electronic band structure and density of states (DOS) for Ac, Th (fcc), and Pa (bct), calculated with (SOC) and without (SR) spin-orbit interaction shown as red solid and black dashed lines, respectively.

C. Lattice dynamical properties

Phonon dispersion and phonon density of states for the three light actinides are shown in Fig. 2 for both SR and SOC calculations. Each spectrum was calculated at the respective optimized structure. As a general trend, the spectra show a hardening with increasing atomic number (from Ac to Pa), which correlates with the decreasing unit-cell volume when the filling of the $5f$-level increases (see Table I). Similarly, because SOC has little influence on the equilibrium volume,
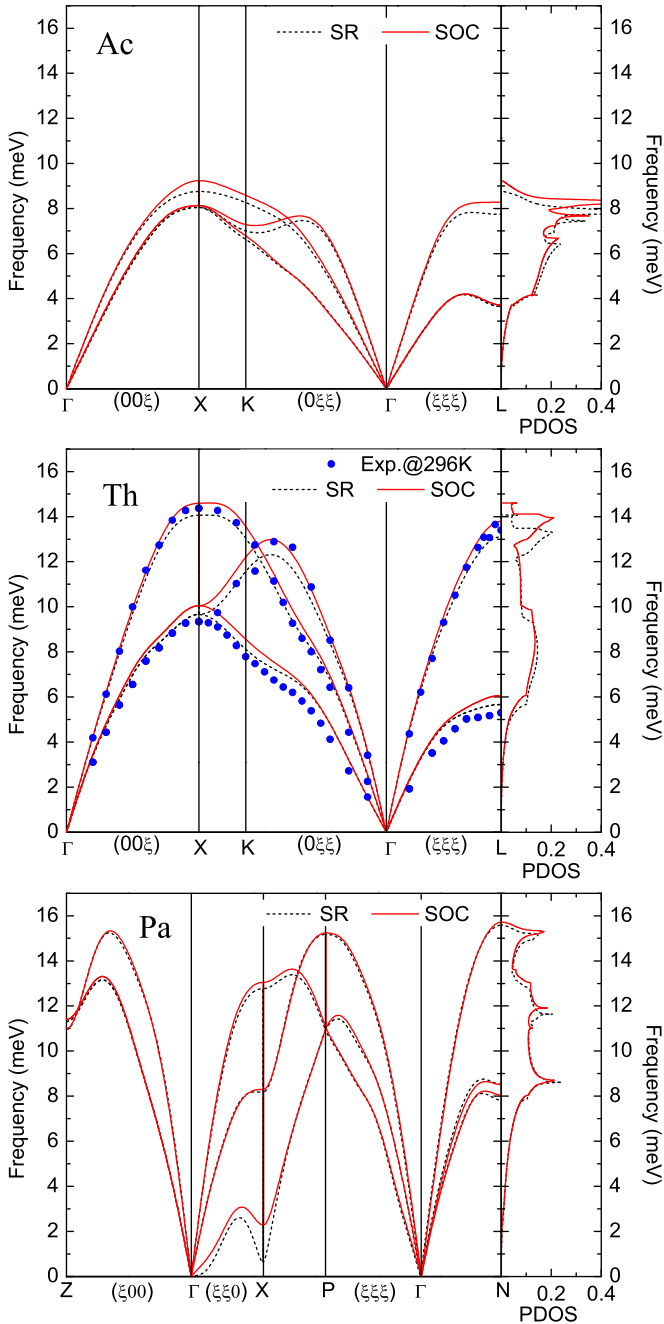
FIG. 2. Phonon dispersion and phonon density of states (PDOS) for Ac, Th (fcc), and PA (bct), for both SR and SOC schemes. For Th, experimental data taken from Ref. [8] are included for comparison (filled symbols).

there are only subtle differences in the phonon dispersion of Ac and Th (less than 1 meV). For both elements, the SOC spectra are slightly harder than for the SR case, which again correlates with a reduced volume. For Pa, dispersion curves from SR and SOC calculations are practically identical, with the exception of a low-frequency transverse mode near the X point. This mode is almost unstable without SOC, but stabilizes when SOC is included.

A closer look at the dispersion curves reveals various anomalous features. Ac displays a weak dip of the transverse

branch along Γ-L close to the zone boundary, while Th shows a weak anomaly along the Γ-K-X high-symmetry direction close to K. For Pa, in addition to the above mentioned low-frequency branch at X, there are a couple of subtle anomalies at the boundary Z and N point (transverse branches). Such phonon anomalies could be a signature of enhanced electron-phonon coupling.

To date, experimental data exist only for the phonon spectrum of Th. These data obtained by inelastic neuron scattering [8] are added in Fig. 2. Our calculated phonon dispersion shows good agreement with the measurements, reproducing even the above mentioned phonon anomaly. This demonstrates that lattice dynamical properties of the light actinides can be calculated reliably within DFPT.

D. Electron-phonon coupling and superconducting properties

In the following, we discuss the electron-phonon interaction and related superconducting properties within a phonon-mediated pairing scenario. As mentioned in Sec. II, e-ph matrix elements can be directly obtained within DFPT and allow a calculation of the isotropic Eliashberg function $\alpha^2 F(\omega)$. Results for Ac, Th, and Pa are shown in Fig. 3 for both SR and SOC calculations. Despite their different lattice structures, Th and Pa exhibit very similar scales for $\alpha^2 F(\omega)$ with respect to both frequency and magnitude. In contrast, $\alpha^2 F(\omega)$ for Ac is visibly larger, while it extends only to about 9 meV due to the softer phonon spectrum.

The changes induced by SOC are quite distinct. For Ac and Pa, SR and SOC spectra are very similar beside a slight hardening for SOC. This contrasts the case of Th, where the Eliashberg function exhibits a clear overall reduction when SOC is turned on. To better understand the reason for such a different behavior, it is useful to take a closer look at the SOC-induced changes of three quantities which determine $\alpha^2 F(\omega)$ [see Eqs. (1)–(3)]. These are (i) the number of electronic states at the Fermi level ($N(E_F)$), (ii) the phonon frequencies, and (iii) electron-phonon coupling matrix elements. Results for $N(E_F)$ are collected in Table II. They show that SOC leads to small changes for Ac (-1%) and Pa ($+2\%$), while a larger reduction of about 10% is found for Th. In order to separate the SOC modifications on the phonon frequencies from those on

TABLE II. Density of states at the Fermi level $N(E_F)$ (states/eV cell^{-1} spin^{-1}), average effective frequency $\omega_{\log}$ (meV), and electron-phonon coupling parameter (λ) for the light-actinides calculated with the SR and SOC schemes. λ values are compared with theoretical results from literature (Theory) [19,20]. Latter values for Pa are put in parenthesis, because they were obtained for the fcc structure.

		Ac (fcc)		Th (fcc)		Pa (bct)	
		SR	SOC	SR	SOC	SR	SOC
This work	$N(E_F)$	1.006	0.992	0.696	0.626	1.248	1.274
	$\omega_{\log}$	5.928	6.087	8.747	9.125	8.442	9.102
	λ	0.972	0.975	0.577	0.456	0.592	0.552
Theory	λ	1.265[a]	1.655[b]	0.529[a]	0.522[b]	(0.268)[a]	(0.279)[b]

[a]Ref. [19].
[b]Ref. [20].
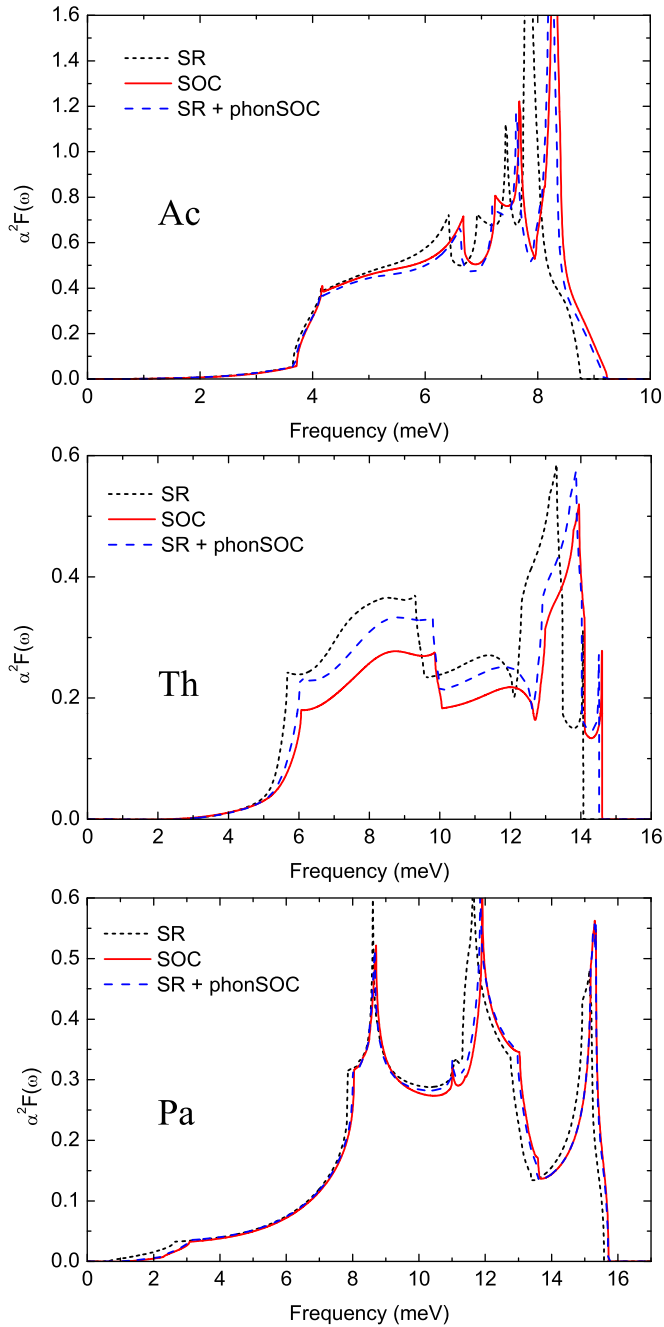
FIG. 3. Eliashberg functions for Ac, Th, and Pa, (note the different scales for each element) comparing the SR, SOC, and the mixed scheme. The latter combines the electronic part and the e-ph matrix elements from the SR scheme with phonons taken from the SOC calculation.

FIG. 4. Evolution of the critical temperature T_c for Ac, Th, and Pa as a function of the Coulomb pseudopotential μ^*, comparing SR and SOC results. Experimental values for Th (1.4 K) [45,46] and Pa (0.43 K) [47] are shown as horizontal dashed lines.

e-ph matrix elements, we evaluated the Eliashberg function in a mixed scheme. Here we combined the electronic quantities as well as the e-ph matrix elements from the SR calculation with phonon frequencies taken from the SOC calculation. Results are also shown in Fig. 3. For Ac, the Eliashberg function obtained by this mixed scheme is virtually identical to the SOC result, indicating that electronic properties and e-ph matrix elements are practically unchanged by SOC. The same is found for Pa. The situation is different for Th, where the SOC

calculation results in a further reduction of the spectrum with respect to the mixed scheme. This shows that for Th changes in the electronic part play a more prominent role.

Results for integral quantities of the Eliashberg functions, like the average coupling constant λ [Eq. (4)] and the average effective frequency $\omega_{\log}$ [Eq. (5)], are also presented in Table II. Following the trend in the Eliashberg function, the e-ph coupling constant λ decreases from Ac to Th and Pa. For Ac, we obtain a value slightly smaller than 1, which is much

lower than previously calculated within the Gaspary-Gyorffi theory [19,20]. Still this represents a sizable coupling strength and puts Ac close to the strong coupling regime. λ practically does not change when SOC is switched on. For Th, SOC leads to a sizable reduction of 21% in λ with respect to the SR calculation, which originates from the reduction of $N(E_F)$ by about 10% combined with a slight hardening of the phonon spectrum. The latter reduces λ by about 7%, as can be deduced from comparing λ_{SR} with the value $\lambda_{\mathrm{mix}} = 0.534$ obtained in the mixed scheme, where SOC is only taken into account for the phonon spectrum. In the case of Pa, SOC reduces λ by 7%, which again is mainly coming from the hardening of the phonon spectrum, as indicated by $\lambda_{\mathrm{mix}} = 0.563$. We note that the small values of less than 0.3 obtained for Pa by Skriver *et al.* [19,20] relate to a fcc structure. To check this, we applied our pseudopotential method to Pa with an fcc structure and also found λ values of the order of 0.2. This shows that the lower crystal symmetry of the bct structure helps to increase λ by a factor 2–3.

Finally, from the calculated $\alpha^2 F(\omega)$ we solved numerically the isotropic Eliashberg gap equations to obtain estimates for the critical temperature T_c [25,37–39]. Figure 4 shows T_c as a function of the single remaining parameter, the Coulomb pseudopotential μ^*. The largest T_c is expected for Ac, which is predicted to lie in the range 4–5 K for typical values of μ^* (0.1–0.13). Following the trends seen for λ in Table II, the influence of SOC on T_c is almost negligible for Ac and Pa, while in the case of Th, it causes a sizable reduction of T_c.

Experimental values of T_c were determined for both Th and Pa and are shown in Fig. 4 as horizontal lines. Comparison with the relativistic calculations shows that the experimental T_c's are reproduced with $\mu^* \approx 0.07$ and $\mu^* \approx 0.17$ for Th and Pa, respectively. These values are falling outside the range of 0.1–0.13 typically expected for simple metals. This could hint to the growing importance of correlations related to the partial filling of $5f$ states, which may be not sufficiently described by GGA. While correlation corrections beyond LDA/GGA are well known to be relevant for various properties of $4f$ and later $5f$ elements, a recent study suggested that they may also be needed to improve the description of the early actinides [48]. Indeed our own calculations of the electronic structure for Th within

the GGA+U+SOC scheme [50] resulted in a shift of the f states such that $N(E_F)$ increased, if the relaxed structure was taken into account. This increase was of the same order as the difference between SR and SOC discussed above, suggesting a similar increase in the coupling. A full calculation of the coupling constant within the GGA+U+SOC scheme is, however, currently not possible.

IV. CONCLUSIONS

We have performed a comprehensive study of the electronic, lattice dynamical, and superconducting properties of the early actinides Ac, Th, and Pa, within a relativistic density functional perturbation approach. Ac is predicted to have the largest e-ph coupling close to 1, and an estimated T_c of the order 4–5 K. This would be the highest transition temperature among the actinides, but experimental verification is pending. Despite different lattice structures, Th and Pa possess very similar coupling strengths, which are, however, significantly smaller than for Ac. A systematic comparison between scalar-relativistic calculations and those including spin-orbit interaction exhibits in all cases a hardening of the phonon spectra, when SOC is included. For Ac and Pa, however, we found only a minor influence of SOC on the pairing properties, while for Th a 21% reduction in λ is obtained, which can be traced back to the splitting of electronic bands and a resulting reduction of the density of states in the vicinity of the Fermi energy. Our finding that experimental T_c's for Th and Pa are not compatible with standard values for μ^*, hints to the need to assess the relevance of correlation corrections beyond standard DFT for the pairing interaction in the presence of partially filled $5f$ states.

[1] H. L. Skriver, O. K. Andersen, and B. Johansson, Phys. Rev. Lett. **41**, 42 (1978).

[2] M. S. S. Brooks, J. Phys. F **13**, 103 (1983).

[3] P. Söderlind, L. Nordström, L. Yongming, and B. Johansson, Phys. Rev. B **42**, 4544 (1990).

[4] P. Söderlind, O. Eriksson, B. Johansson, and J. M. Wills, Phys. Rev. B **50**, 7291 (1994).

[5] J. Kollár, L. Vitos, and H. L. Skriver, Phys. Rev. B **55**, 15353 (1997).

[6] M. D. Jones, J. C. Boettger, R. C. Albers, and D. J. Singh, Phys. Rev. B **61**, 4644 (2000).

[7] J. Kuneš, P. Novák, R. Schmid, P. Blaha, and K. Schwarz, Phys. Rev. B **64**, 153102 (2001).

[8] R. A. Reese, S. K. Sinha, and D. T. Peterson, Phys. Rev. B **8**, 1332 (1973).

[9] W. P. Crummett, H. G. Smith, R. M. Nicklow, and N. Wakabayashi, Phys. Rev. B **19**, 6028 (1979).

[10] M. E. Manley, B. Fultz, R. J. McQueeney, C. M. Brown, W. L. Hults, J. L. Smith, D. J. Thoma, R. Osborn, and J. L. Robertson, Phys. Rev. Lett. **86**, 3076 (2001).

[11] M. E. Manley, G. H. Lander, H. Sinn, A. Alatas, W. L. Hults, R. J. McQueeney, J. L. Smith, and J. Willit, Phys. Rev. B **67**, 052302 (2003).

[12] J. Wong, M. Krisch, D. L. Farber, F. Occelli, A. J. Schwartz, T. C. Chiang, M. Wall, C. Boro, and R. Xu, Science **301**, 1078 (2003).

[13] S. Baroni, S. de Gironcoli, and A. Dal Corso, Rev. Mod. Phys. **73**, 515 (2001).

[14] J. Bouchet and G. Jomard, J. Alloys Compd. **444**, 271 (2003).

[15] J. Bouchet, F. Jollet, and G. Zérah, Phys. Rev. B **74**, 134304 (2006).

[16] C. E. Hu, Z. Y. Zeng, L. Zhang, X. R. Chen, and L. C. Cai, Solid State Commun. **150**, 393 (2010).

[17] P. Souvatzis, T. Bjorkman, O. Eriksson, P. Andersson, M. I. Katsnelson, and S. P. Rudin, J. Phys.: Condens. Matter **21**, 175402 (2009).

[18] P. Söderlind, J. Electron Spectrosc. Relat. Penom. **194**, 81 (2014).

[19] H. L. Skriver and I. Mertig, Phys. Rev. B **32**, 4431 (1985).

[20] H. L. Skriver, O. Eriksson, I. Mertig, and E. Mrosan, Phys. Rev. B **37**, 1706 (1988).

[21] W. L. McMillan, Phys. Rev. **167**, 331 (1968).

[22] M. S. S. Brooks, B. Johansson, and H. L. Skriver, *Handbook on the Physics and Chemistry of The Actinides*, edited by A. J. Freeman and G. Lander (North-Holland, Amsterdam, 1984).

[23] W. John, V. V. Nemoshkalenko, V. N. Antonov, and Vl. N. Antonov, Phys. Status Solidi B **121**, 233 (1984).

[24] J. W. Kohn and L. J. Sham, Phys. Rev. **140**, A1133 (1965).

[25] G. M. Eliashberg, Sov. Phys. JETP **11**, 696 (1960).

[26] S. G. Louie, K. M. Ho, and M. L. Cohen, Phys. Rev. B **19**, 1774 (1979).

[27] B. Meyer, C. Elsässer, and M. Fähnle, *FORTRAN90 Program for Mixed-Basis Pseudopotential Calculations for Crystals*, Max-Planck-Institut für Metallforschung, Stuttgart (unpublished).

[28] R. Heid, K. P. Bohnen, I. Y. Sklyadneva, and E. V. Chulkov, Phys. Rev. B **81**, 174527 (2010).

[29] I. Y. Sklyadneva, R. Heid, P. M. Echenique, K. B. Bohnen, and E. V. Chulkov, Phys. Rev. B **85**, 155115 (2012).

[30] D. Vanderbilt, Phys. Rev. B **32**, 8412 (1985).

[31] R. Heid and K. P. Bohnen, Phys. Rev. B **60**, R3709 (1999).

[32] R. Heid, K. P. Bohnen, and K. M. Ho, Phys. Rev. B **57**, 7407 (1998).

[33] O. De la Peña-Seaman, R. Heid, and K. P. Bohnen, Phys. Rev. B **86**, 184507 (2012).

[34] J. P. Perdew, K. Burke, and M. Ernzerhof, Phys. Rev. Lett. **77**, 3865 (1996).

[35] Ground-state structural and phonon dispersion calculations for Th performed with LDA (PW92) for the exchange-correlation functional gave significantly worse results than GGA. The LDA equilibrium volume was 10% smaller than experimental data, while the phonon spectra was approx. 9% harder as compared to inelastic neutron scattering data.

[36] C.-L. Fu and K. M. Ho, Phys. Rev. B **28**, 5480 (1983).

[37] J. P. Carbotte, Rev. Mod. Phys. **62**, 1027 (1990).

[38] V. Z. Kresin and S. A. Wolf, Phys. Rev. B **46**, 6458 (1992).

[39] S. Y. Savrasov, D. Y. Savrasov, and O. K. Andersen, Phys. Rev. Lett. **72**, 372 (1994).

[40] J. D. Farr, A. L. Giorgi, M. G. Bowman, and R. K. Money, J. Inorg. Nucl. Chem. **18**, 42 (1961).

[41] D. S. Evans and G. V. Raynor, J. Nucl. Mater. **1**, 281 (1959).

[42] G. Bellussi, U. Benedict, and W. B. Holzapfel, J. Less-Common Met. **78**, 147 (1981).

[43] W. H. Zachariasen, Acta Crystallogr. **5**, 19 (1952).

[44] U. Benedict, J. C. Spirlet, C. Dufour, I. Birkel, W. B. Holzapfel, and J. R. Peterson, J. Magn. Magn. Mater. **29**, 287 (1982).

[45] W. R. Decker and D. K. Finnemore, Phys. Rev. **172**, 430 (1968).

[46] B. A. Haskell, W. J. Keeler, and D. K. Finnemore, Phys. Rev. B **5**, 4364 (1972).

[47] J. L. Smith, J. C. Spirlet, and W. Müller, Science **205**, 188 (1979).

[48] A. V. Lukoyanov, M. O. Zaminev, and V. I. Anisimov, JETP **118**, 148 (2014).

[49] We employed the Wien2K code, with a muffin-tin radius of 2.80 a.u., using a $R_{MT} \times K_{MAX} = 9.5$, and $16 \times 16 \times 16 k$-point mesh, where the potential and charge density were expanded in crystal harmonics up to $l = 12$.

[50] GGA+U+SOC calculations were performed with the Wien2K code employing $U = 2.3$ eV and $J = 0.41$ eV for the $5f$-states following Ref. [48].